Author(s): Leonov, G.A.; Kuznetsov, Nikolay; Yuldashev, Marat; Yuldashev, Renat

Title: Nonlinear dynamical model of Costas loop and an approach to the analysis of its stability in the large

Year: 2015

Version:

CrossMark

Nonlinear dynamical model of Costas loop and an approach to the analysis of its stability in the large

G.A. Leonov [a], N.V. Kuznetsov [a,b,*], M.V. Yuldashev [a,b], R.V. Yuldashev [a,b]

[a] Saint-Petersburg State University, Russia
[b] University of Jyväskylä, Finland

A B S T R A C T

The analysis of the stability and numerical simulation of Costas loop circuits for high-frequency signals is a challenging task. The problem lies in the fact that it is necessary to simultaneously observe very fast time scale of the input signals and slow time scale of phase difference between the input signals. To overcome this difficult situation it is possible, following the approach presented in the classical works of Gardner and Viterbi, to construct *a mathematical model of Costas loop*, in which only slow time change of signal's phases and frequencies is considered. Such a construction, in turn, requires the computation of phase detector characteristic, depending on the waveforms of the considered signals. While for the stability analysis of the loop near the locked state (local stability) it is usually sufficient to consider the linear approximation of phase detector characteristic near zero phase error, the global analysis (stability in the large) cannot be accomplished using simple linear models.

The present paper is devoted to the rigorous construction of nonlinear dynamical model of classical Costas loop, which allows one to apply numerical simulation and analytical methods (various modifications of absolute stability criteria for systems with cylindrical phase space) for the effective analysis of stability in the large. Here a general approach to the analytical computation of phase detector characteristic of classical Costas loop for periodic non-sinusoidal signal waveforms is suggested. The classical ideas of the loop analysis in the signal's phase space are developed and rigorously justified. Effective analytical and numerical approaches for the nonlinear analysis of the mathematical model of classical Costas loop in the signal's phase space are discussed.

1. Introduction

The Costas loop [1,2] is a classical phase-locked loop (PLL) based circuit for carrier recovery. Nowadays among the applications of Costas loop there are Global Positioning Systems (see, e.g., [3–7]), wireless communication (see, e. g., [8–14] and others [15–23].

* Corresponding author at: University of Jyväskylä, Finland.
E-mail address: nkuznetsov239@gmail.com (N.V. Kuznetsov).

A PLL-based circuit behaves as a nonlinear control system and its *physical model in the signal space* can be described by nonlinear nonautonomous difference or differential equations. In practice, numerical simulation is widely used for the analysis of nonlinear PLL-based models (see, e.g., [24–28]). However the explicit numerical simulation of the *physical model* of Costas loop or its *mathematical model in the signal space* (e.g., full SPICE-level simulation) is rather complicated for the high-frequency signals. The problem lies in the fact that it is necessary to consider simultaneously both very fast time

scale of the signals and slow time scale of phase difference between the signals, so one very small simulation time-step needs to be taken over a very long total simulation period [29–31].

To overcome this difficult situation it is possible, following the approach presented, e.g., in the classical works of Gardner and Viterbi, to construct *a mathematical model in the signal's phase space*, in which only slow time change of signal's phases and frequencies is considered. Such a construction, in turn, requires the computation of phase detector characteristic, which depends on PD physical realization and the waveforms of the considered signals [32–35]. Note that "*understanding how phase detectors work is one of the major keys to understanding how PLLs work*" [36].

Nowadays the following scheme

1. consideration of the *physical model in the signal space*;
2. computation of phase detector characteristic and the construction of the *mathematical model in the signal's phase space* (phase-domain macromodel [29]);
3. nonlinear analysis of the transient processes of the signal's phases adjustment and the estimation of the dependence of various important acquisition characteristics on circuit's parameters in the *mathematical model in the signal's phase space* by numerical and analytical methods,

which goes back to pioneering works on PLL and considered below in the paper, is widely used [29,37] (see, e.g., modern engineering literature [25–28,36,38–47] and others). Such an approach allows one to analyze effectively the transient processes of signal's phases adjustment and to estimate the dependence of many important acquisition characteristics on circuit's parameters by numerical and analytical methods. It is important to note that the construction of *mathematical model* and the use of results of its analysis for the conclusions on the behavior of the considered *physical model* are needed for rigorous mathematical foundation [35,48], but it is often ignored in engineering studies. The attempts to justify analytically the reliability of conclusions, based on simplified engineering approaches, and rigorous study of nonlinear models are quite rare (see, e.g., [49–61]).

In the present paper a general effective approach to analytical computation of phase detector characteristic is presented; the classical ideas of analysis and design of PLL-based circuits in the signal's phase space are developed and rigorously justified; for various non-sinusoidal waveforms of high-frequency signals (see, e.g., various applications of

PLL-based circuits with non-sinusoidal signals in [62–68]) its phase-detector characteristics are obtained for the first time and its dynamical model is constructed.

2. Physical model of Costas loop in the signal space

Various modifications of analog and digital Costas loops and PLL with squarer are widely used for BPSK (Binary Phase Shift Keying) and QPSK (Quadrature Phase Shift Keying) demodulation in telecommunication. Because the realization of squaring circuits can be quite difficult, the Costas loop is the preferred variant [26]. In digital circuits, the maximum data rate is limited by a speed of ADC (Analog-to-Digital Converter). In the following classical analog Costas loop, used for BPSK demodulation (similar analysis can also be done for QPSK Costas loop), is considered.

Consider the Costas loop operation (see Fig. 1) with the sinusoidal carrier and VCO (Voltage-Controlled Oscillator) signals with the same frequencies after transient processes. The input signal is BPSK signal, which is a product of the transferred data $m(t) = \pm 1$ and the harmonic carrier $\sin(\omega t)$ with the high frequency ω. Since here the Costas loop in lock is considered, VCO signal is synchronized with the carrier (i.e. there is no phase difference between VCO signal and input carrier). On the lower branch (Q branch) after the multiplication of VCO signal, shifted by 90°, and the input signal by the multiplier block ($\otimes$) one has

$$Q = \tfrac{1}{2}(m(t)\,\sin(0) - m(t)\,\sin(2\omega t)) = -\tfrac{1}{2}m(t)\,\sin(2\omega t). \quad (1)$$

From an engineering point of view, the high-frequency part $\sin(2\omega t)$ in (1) is removed by a low-pass filter on Q branch. Thus, after filtration a signal on Q branch is zero (a constant in the general case when the initial frequencies are different).

On the upper branch (I) the input signal is multiplied by the output signal of VCO:

$$I = \tfrac{1}{2}(m(t)\,\cos(0) - m(t)\,\cos(2\omega t))$$
$$= \tfrac{1}{2}(m(t) - m(t)\,\cos(2\omega t)). \quad (2)$$

The high-frequency term $\cos(2\omega t)$ is filtered by a low-pass filter. Thus, on the upper branch I after filtration one can obtain the demodulated data $m(t)$.

Then both branches are multiplied together and after an additional filtration one gets the signal $g(t)$ to adjust VCO frequency to the frequency of input carrier signal. After a transient process there is no phase difference and the control input of VCO is zero. In the general case when the initial
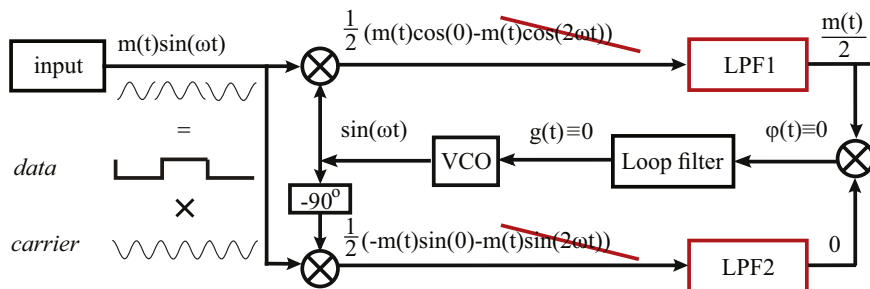

Fig. 1. Costas loop is in lock: $m(t)$ is a useful information (± 1); ω is a frequency of input carrier and VCO output; $m(t)\,\sin(\omega t)$ is an input signal.
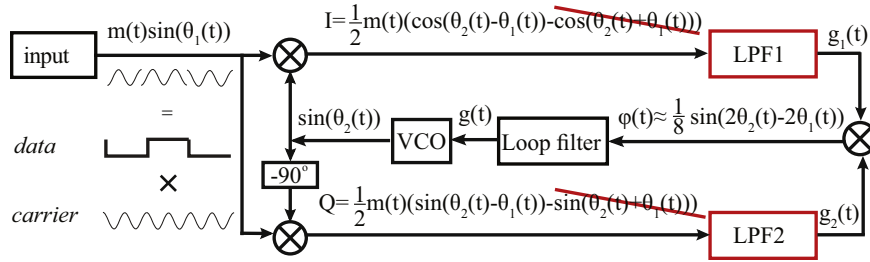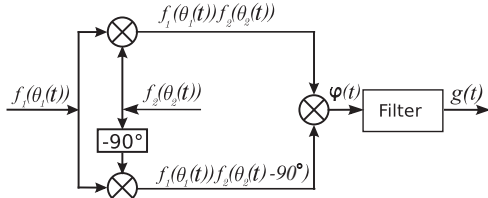
Fig. 2. Costas loop. Operation in the general case.

Fig. 3. Block diagram of simplified Costas loop.

frequencies are different the control input of VCO is constant:

$$g(t) \approx const. \tag{3}$$

Consider the case (see Fig. 2) when the phase of the input carrier $\theta_1(t)$ and the phase of VCO $\theta_2(t)$ are different. The latter means that either (1) the frequencies are different or (2) the frequencies are the same but there is a constant phase difference. For engineers it is a well-known fact [69] that in the considered case of sinusoidal signals the input of loop filter can be approximated as

$$\varphi(t) \approx \tfrac{1}{8} \sin \left(2\theta_2(t) - 2\theta_1(t)\right).$$

This approximation depends on the phase difference of signals and is called a phase detector characteristic of Costas loop for sinusoidal signals. When the phase difference of signals is small, using the linearization $\varphi(t) \approx K(\theta_2(t) - \theta_1(t))$, one can consider a linearized mathematical model of Costas loop for sinusoidal signals (see details in Section 4). This allows one to estimate approximately acquisition parameters by the same methods that were developed for the analysis and design of classical PLLs (see, e.g., [69–72] and others).

In the next section a rigorous mathematical approach to the analytical computation of phase detector characteristic and the nonlinear analysis of classical Costas loop for non-sinusoidal waveforms is considered.

2.1. Simplified model of Costas loop

The low-pass filters on the upper and the lower branches of Costas loop (Fig. 2) are responsible for demodulation process (see Fig. 1) and therefore they can be applied separately from the loop (see, e.g., [4]). From a point of view of the analysis of stability, the filter at the input of VCO executes their filtering functions.

Thus one can consider a simplified physical open-loop model of Costas loop (Fig. 3) with only one filter at the input of VCO. In this case the transmitted data $m(t)$ can be omitted (i.e. $m(t) \equiv 1$) because after the multiplication of

the upper and the lower branches at the input of filter the data are squared: $(m(t)^2 = (\pm 1)^2 = 1)$. Here the signal $f_1(t) = f_1(\theta_1(t))$ represents the carrier and $\theta_1(t)$ represents its phase. In analogy, $f_2(t) = f_2(\theta_2(t))$ represents the output signal of VCO, and $\theta_2(t)$ represents its phase. The functions $f_{1,2}(\theta)$ are called waveforms.

Consider the analysis of Costas loop for general periodic signal waveforms. Suppose that the waveforms $f_{1,2}(\theta)$ are bounded 2π-periodic piecewise differentiable functions[1] (this is true for the most considered waveforms, e.g., sinusoidal, squarewave, sawtooth, triangular, and polyharmonic). Consider the following Fourier series representation:

$$f_p(\theta) = \sum_{i=1}^{\infty} \left(a_i^p \cos(i\theta) + b_i^p \sin(i\theta)\right), \quad \theta \geq 0$$

$$a_i^p = \frac{1}{\pi} \int_{-\pi}^{\pi} f_p(\theta) \cos(i\theta) \, d\theta,$$

$$b_i^p = \frac{1}{\pi} \int_{-\pi}^{\pi} f_p(\theta) \sin(i\theta) \, d\theta, \quad p = 1, 2.$$

The relation between the input $\varphi(t)$ and the output $g(t)$ of linear filter is as follows [73]:

$$g(t) = \alpha_0(t) + \int_0^t \gamma(t-\tau)\varphi(\tau) \, d\tau, \tag{4}$$

where $\gamma(t)$ is an impulse response function of filter and $\alpha_0(t)$ is an exponentially damped function depending on the initial state of filter at $t = 0$.

By (4) the filter output $g(t)$ has the form

$$g(t) = \alpha_0(t) + \int_0^t \gamma(t-\tau)f_1(\theta_1(\tau))f_2(\theta_2(\tau))$$

$$f_1(\theta_1(\tau))f_2\left(\theta_2(\tau) - \frac{\pi}{2}\right)d\tau. \tag{5}$$

2.2. High-frequency signals

For solving the above problem, posed by D. Abramovitch, and applying the averaging methods it is necessary to consider mathematical properties of high-frequency signals. Here an approach is applied and used which is developed for the study of the classical PLL [32,35,48,74].

---

[1] The functions with a finite number of jump discontinuity points differentiable on their continuity intervals.

A high-frequency property of signals can be reformulated in the following way. Suppose that for the frequencies[2]

$$\omega_{1,2}(t) = \dot{\theta}_{1,2}(t), \tag{6}$$

there exist a sufficiently large number ω_{min} such that on a fixed time interval $[0, T]$, where T is independent of ω_{min}, the conditions

$$\omega_{1,2}(t) \geq \omega_{min} > 0 \tag{7}$$

are satisfied. The frequency difference is assumed to be uniformly bounded:

$$|\omega_1(t) - \omega_2(t)| \leq \omega_\Delta^{max}, \quad \forall t \in [0, T]. \tag{8}$$

Requirements (7) and (8) are obviously satisfied for the tuning of two high-frequency oscillators with close frequencies. Let us introduce $\delta = \omega_{min}^{-1/2}$. Consider the relations

$$|\omega_p(t) - \omega_p(\tau)| \leq \Omega, \quad p = 1, 2,$$
$$|t - \tau| \leq \delta, \quad \forall t, \ \tau \in [0, T], \tag{9}$$

where Ω is independent of δ. Conditions (7)–(9) mean that the functions $\omega_p(\tau)$ are almost constant and the functions $f_p(\theta_p(t))$ are rapidly oscillating time functions on the small intervals $[t, t+\delta]$.

To study the filtration of high-frequency signals by filter (4) it is assumed that the impulse response function of filter is a differentiable function with a bounded derivative (this is true for the most considered filters [73]). The boundedness of derivative of $\gamma(t)$ implies that

$$|\gamma(\tau) - \gamma(t)| = O(\delta), \quad |t - \tau| \leq \delta, \ \forall \tau, \ t \in [0, T]. \tag{10}$$

3. Analytical computation of phase detector characteristics for non-sinusoidal waveforms

Consider a block diagram in Fig. 4. Here PD is a non-linear block (describing the operation of all intermediate elements in Fig. 3 between inputs and filter) and its output is 2π-periodic function $\varphi(\theta_2(t) - \theta_1(t))$ (the phase detector characteristic of Costas loop); $G(t)$ is the output of filter.

Suppose that the characteristics and the initial state of filters in Fig. 3 and in Fig. 4 coincide. By (4) the output has the form

$$G(t) = \alpha_0(t) + \int_0^t \gamma(t - \tau)\varphi(\theta_2(\tau) - \theta_1(\tau)) \, d\tau. \tag{11}$$

Theorem 1. *Consider 2π-periodic function $\varphi(\theta)$ of the form*

$$\varphi(\theta) = \frac{A_0^1 A_0^2}{4} + \frac{1}{2} \sum_{l=1}^{\infty} \left(\left(A_l^1 A_l^2 + B_l^1 B_l^2\right) \cos(l\theta) \right.$$
$$\left. + (A_l^1 B_l^2 - B_l^1 A_l^2) \sin(l\theta) \right), \tag{12}$$

where the coefficients A_l^p and B_l^p are expressed via the

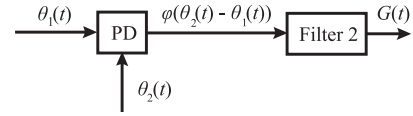**Fig. 4.** Phase detector (PD) of Costas loop and filter.

coefficients of the waveforms $f_{1,2}(\theta)$ in the following way:

$$A_l^1 = \frac{a_0^1 a_l^1}{2} + \frac{1}{2} \sum_{m=1}^{\infty} \left[a_m^1 (a_{m+l}^1 + a_{m-l}^1) + b_m^1 \left(b_{m+l}^1 + b_{m-l}^1\right) \right],$$

$$B_l^1 = \frac{a_0^1 b_l^1}{2} + \frac{1}{2} \sum_{m=1}^{\infty} \left[a_m^1 \left(b_{m+l}^1 - b_{m-l}^1\right) - b_m^1 (a_{m+l}^1 - a_{m-l}^1) \right],$$

$$A_l^2 = \frac{a_0^2 \alpha_l^2}{2} + \frac{1}{2} \sum_{m=1}^{\infty} \left[\alpha_m^2 (\alpha_{m+l}^2 + \alpha_{m-l}^2) + \beta_m^2 \left(\beta_{m+l}^2 + \beta_{m-l}^2\right) \right],$$

$$B_l^2 = \frac{a_0^2 \beta_l^2}{2} + \frac{1}{2} \sum_{m=1}^{\infty} \left[\alpha_m^2 \left(\beta_{m+l}^2 - \beta_{m-l}^2\right) - \beta_m^2 (\alpha_{m+l}^2 - \alpha_{m-l}^2) \right], \tag{13}$$

and

$$\alpha_k^2 = \begin{cases} a_k^2, & k = 4p, \\ b_k^2, & k = 4p+1, \\ -a_k^2, & k = 4p+2, \\ -b_k^2, & k = 4p+3, \end{cases} \quad \beta_k^2 = \begin{cases} b_k^2, & k = 4p, \\ -a_k^2, & k = 4p+1, \\ -b_k^2, & k = 4p+2, \\ a_k^2, & k = 4p+3. \end{cases} \tag{14}$$

If high-frequency conditions (7)–(9) and condition on filter (10) are satisfied, then the relation

$$|g(t) - G(t)| = O(\delta), \quad \forall t \in [0, T] \tag{15}$$

is valid.

In other words, this theorem separates the low-frequency error-correcting signal from parasitic high-frequency oscillations and proves that the considered function $\varphi(\theta)$ is a phase detector characteristic of Costas loop. Thus the filter input can be approximated by the function $\varphi(\theta)$ in the sense that a change in the filter output signal is sufficiently small (see (15)).

For sinusoidal waveforms this fact was known to engineers [2] without rigorous justification.

Remark 1. Since $f_{1,2}(\theta)$ are piecewise-differentiable, then

$$A_k^{1,2} = O\left(\frac{1}{k}\right), \quad B_k^{1,2} = O\left(\frac{1}{k}\right), \tag{16}$$

and $\varphi(\theta)$ is a smooth function.

Remark 2. For the most considered waveforms, infinite series (12) can be truncated up to the first $\sqrt{\omega_{min}}$ terms. By (13) and (16), the remainder $R_{[1/\delta]}$ of series (12) can be estimated as

$$|R_{[1/\delta]}(x)| \leq O\left(\sum_{l=[1/\delta]+1}^{\infty} \frac{1}{l^2} \right) \leq O(\delta).$$

$f_{1,2}(\theta) = \sin(\theta), \quad \varphi(\theta) = -\frac{1}{8}\sin(2\theta)$

$f_{1,2}(\theta) = -\frac{2}{\pi}\sum_{n=1}^{\infty}\frac{1}{n}\sin(n\theta),$

$$\varphi(\theta) = \frac{-1}{72} + \frac{1}{2}\sum_{l=1}^{\infty}\begin{cases}\frac{16}{\pi^4 l^4}\cos(l\theta), \quad l = 4p, \quad p \in \mathbb{N}_0 \\[4pt] \frac{-4(\pi l-2)}{\pi^4 l^4}\cos(l\theta)\frac{-4(\pi l-2)}{\pi^4 l^4}\sin(l\theta), \\ \qquad l = 4p+1, \\[4pt] \frac{-8}{\pi^3 l^3}\sin(l\theta), \quad l = 4p+2, \\[4pt] \frac{4(\pi l+2)}{\pi^4 l^4}\cos(l\theta)\frac{-4(\pi l+2)}{\pi^4 l^4}\sin(l\theta), \\ \qquad l = 4p+3,\end{cases}$$

$f_{1,2}(\theta) = \frac{8}{\pi^2}\sum_{n=1}^{\infty}\frac{1}{(2n-1)^2}\cos((2n-1)\theta)$

$\varphi(\theta) = \frac{512}{\pi^5}\sum_{l=1}^{\infty}\frac{1}{(4l+2)^5}\sin((4l+2)\theta)$

$f_1(\theta) = \frac{8}{\pi^2}\sum_{n=1}^{\infty}\frac{1}{(2n-1)^2}\cos((2n-1)\theta)$

$f_2(\theta) = -\frac{2}{\pi}\sum_{n=1}^{\infty}\frac{1}{n}\sin(n\theta)$

$$\varphi(\theta) = \frac{-1}{72} + \frac{8}{\pi^2}\sum_{l=1}^{\infty}\begin{cases}\frac{4}{\pi^2(l+4)^4}\cos((l+4)\theta), \quad l = 4p, \\[4pt] -\frac{2}{\pi l^3}\sin(l\theta), \quad l = 4p+2, \\[4pt] 0, \quad l = 2p+1, \quad p \in \mathbb{N}_0\end{cases}$$

$f_1(\theta) = -\frac{2}{\pi}\sum_{n=1}^{\infty}\frac{1}{n}\sin(n\theta)$

$f_2(\theta) = \frac{8}{\pi^2}\sum_{n=1}^{\infty}\frac{1}{(2n-1)^2}\cos((2n-1)\theta)$

$\varphi(\theta) = \sum_{l=0}^{\infty}\frac{128}{\pi^5(4l+2)^5}\sin((4l+2)\theta),$
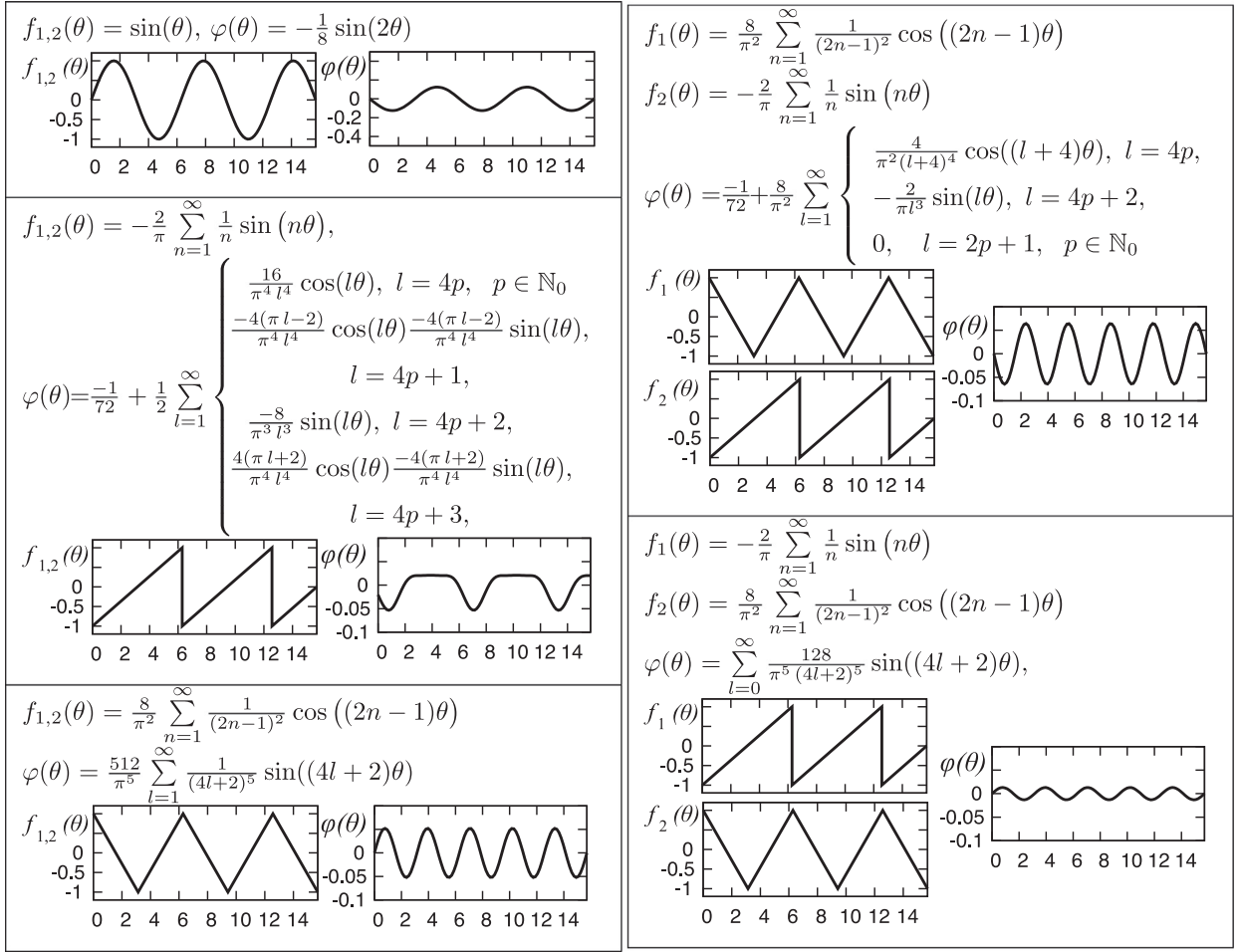
The theorem allows one to compute a phase detector characteristic[3,4] for the following typical signals given below in the table.

4. Description of classical Costas loop in the signal's phase space

From a mathematical point of view, linear filter (4) can also be described by a system of linear differential equations

$$\dot{\mathbf{x}} = \mathbf{A}\mathbf{x} + \mathbf{b}\varphi(t), \quad \sigma = \mathbf{c}^*\mathbf{x}, \qquad (17)$$

a solution of which has the form (4). Here $\mathbf{A}$ is a constant matrix, $\mathbf{x}(t)$ is the state vector of Filter, $\mathbf{b}$ and $\mathbf{c}$ are constant vectors. The model of VCO is usually assumed to be linear:

$$\dot{\theta}_2(t) = \omega_{free} + LG(t), \quad t \in [0, T], \qquad (18)$$

---

[3] It can be proved that the phase detector characteristic for Costas loop in Fig. 2 coincides with (12) under some essential conditions on frequency characteristics of filters on the upper and lower branches.
[4] Since there is an integration in VCO model (18), for the case of proportional-integrating filter one can easily prove an analog of the theorem with the estimation $|\int_0^t G(t) - \int_0^t g(t)| = O(\delta)$.

where ω_{free} is the free-running frequency of VCO and L is the gain of VCO. Similarly, one can consider various nonlinear models of VCO (see, e.g., [37]). Therefore the initial VCO frequency is as follows:

$$\dot{\theta}_2(0) = \omega_{free} + L\mathbf{c}^*\mathbf{x}(0).$$

By equations of filter (17) and VCO (18) one has

$$\dot{\mathbf{x}} = \mathbf{A}\mathbf{x} + \mathbf{b}f_1(\theta_1(t))f_2(\theta_2(t))f_1(\theta_1(t))f_2\left(\theta_2(t) - \frac{\pi}{2}\right),$$
$$\dot{\theta}_2 = \omega_{free} + L\mathbf{c}^*\mathbf{x}. \qquad (19)$$

Nonautonomous system (19) describes *physical model of Costas loop in the signal space* (see Fig. 5) and is rather difficult for the study.

Suppose that the frequency of reference signal is a constant

$$\dot{\theta}_1(t) \equiv \omega_1. \qquad (20)$$

Then Theorem 1 allows one to consider more simple autonomous system of differential equations (in place of nonautonomous (19)), which describes the mathematical model of Costas loop in the signal's phase space:

$$\dot{\mathbf{x}} = \mathbf{A}\mathbf{x} + \mathbf{b}\varphi(\theta_\Delta), \quad \dot{\theta}_\Delta = \omega_{free} - \omega_1 + L\mathbf{c}^*\mathbf{x},$$
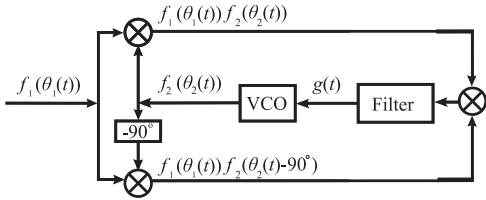$$\theta_\Delta = \theta_2 - \theta_1. \qquad (21)$$

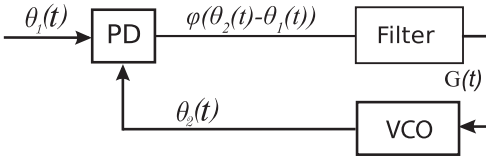**Fig. 5.** Block diagram of Costas loop in the signal space.

Fig. 6. Block diagram of Costas loop in the signal's phase space.

Here the initial difference of frequencies (at $t=0$) has the form $\dot{\theta}_\Delta(0) = \omega_{free} - \omega_1 + L\mathbf{c}^*\mathbf{x}(\mathbf{0})$.[5]

The well-known averaging method permits[6] to show that the solutions of (19) and (21) are close on time interval $[0, T]$, where $T \ll \omega_{min}$, under some assumptions [75,76]. Thus the block diagram of Costas loop in the signal space (Fig. 5) can be asymptotically changed (for high-frequency generators, see conditions (7)–(10)) to the block diagram in the signal's phase space (Fig. 6). Here PD has the corresponding characteristics (12).

Linearized model (21), where $\varphi(\theta_\Delta)$ is changed to $K\theta_\Delta$, may be used for analysis in the case when the considered circuit "*is in lock, but analysis of the acquisition behavior cannot be accomplished using the simple linear models and nonlinear analysis techniques are necessary*" [28]. Note that the linearization and the analysis of linearized models of control systems may result in incorrect conclusions,[7] so one can read in [37] "*the use of linear macromodels can lead to qualitatively incorrect prediction of important PLL phenomena*". At the same time the attempts to justify analytically the reliability of conclusions, based on simplified engineering approaches, and rigorous study of nonlinear models are quite rare and one of the reasons is that "*nonlinear analysis techniques are well beyond the scope of most undergraduate courses in communication theory*" [28].

While the physical model of Costas loop in the signal space (19) is nonautonomous and its rigorous global analysis (transient processes, stability in the large, cycle slipping, etc.) is rather difficult and creative task, for the global analysis of nonlinear autonomous model (21) of Costas loop, the well-known methods of analysis of

pendulum-like systems can be applied (see, e.g., [79,54,80, 56,81,60]). Modification of direct Lyapunov method with the construction of periodic Lyapunov-like functions, the method of positively invariant cone grids, and the method of nonlocal reduction turned out to be most effective [82,83,80,81]. The last method, which combines the elements of direct Lyapunov method and bifurcation theory, allows one to extend the classical results of Tricomi [84] and his progenies to the multidimensional dynamical systems [83,85].

5. Simulation of Costas loop

Since in the block diagram in Fig. 6 and system (21) only slow time change of signal's phases and frequencies is considered, they can be effectively studied numerically.

For the simulation of system (21) with the function $\varphi(\cdot)$ of the form (12), in place of conditions (8) and (10) the conditions $|\omega_\Delta^{max}| \ll \omega_{min}$, $|\lambda_{\mathbf{A}}| \ll \omega_{min}$ should be considered, where $\lambda_{\mathbf{A}}$ is the largest (in modulus) eigenvalue of matrix A. Also, it is necessary to consider $T \ll \omega_{min}$ to justify the transition from Eqs. (35)–(39) (see Appendix) and to use Remark 1.

The considered theoretical results are justified by the simulation[8,9] of those considered in the previous section of Costas loop models in the signal and signal's phase spaces. In Fig. 7 are shown the transient processes of VCO input in block diagrams in Figs. 5 and 6 (here it is important if and when VCO input becomes a constant, see (3)).

Here the simulation in the signal's phase space is more than 100 times faster. Unlike the filter output in the signal's phase space, in the signal space the filter output contains additional high-frequency oscillation. These high-frequency oscillations interfere with qualitative analysis and efficient simulation of Costas loop. The passage to the analysis of autonomous dynamical model of Costas loop (in place of the nonautonomous one) allows one to overcome the difficulties that relate to the analysis of Costas loop in the signal space.

The approach described can be adapted to digital Costas loops [4,88], where the filter and the VCO are digital unlike those in Fig. 5. If a discretization step is sufficiently small, then a digital filter acts similar to an analog filter. In this case it can be shown that the considered mathematical model in the signal's phase space is adequate (see Fig. 8).

In conclusion it should be remarked that in the signal's phase space a similar numerical simulation of the whole transient process (around 10 s – see Fig. 7) of Costas loop with frequencies around 1 GHz = 10^9 Hz takes less than 1 s. At the same time to perform the accurate simulation of Costas loop in the signal space for such frequencies one has to use a discretization step much less than 10^{-9}, what results in a very long simulation time to oversee the whole transient process: during 10 s of simulation in the signal

---

[5] Note that to consider one-dimensional stability domains, e.g., defined by $\omega_\Delta = \omega_1 - \omega_{free}$, one has to assume that $c^*x(0) = 0$. In the general case one has to consider multi-dimensional stability domains taking into account the initial state of loop filter — vector $x(0)$.

[6] Note that the derivation of dynamical model (21) and the rigorous justification of its adequacy for the analysis of stability are possible here only under condition (20), while formula (12) is obtained for PD characteristic in the general case without condition (20).

[7] See also counterexamples to the filter hypothesis, Aizerman's and Kalman's conjectures on the absolute stability of nonlinear control systems [77], and the Perron effects of the largest Lyapunov exponent sign inversions [78], etc.

---

[8] One can compare the numerical integration of systems (19) and (21) with the simulation of realization of block diagrams in Figs. 5 and 6, f.e., in Matlab Simulink (see, e.g., [28,86] and the patent application [87]).

[9] While we consider a very simple filter, sawtooth and triangle waveforms in simulation, one can consider similar effects for lag-lead or PI filters and other waveforms.
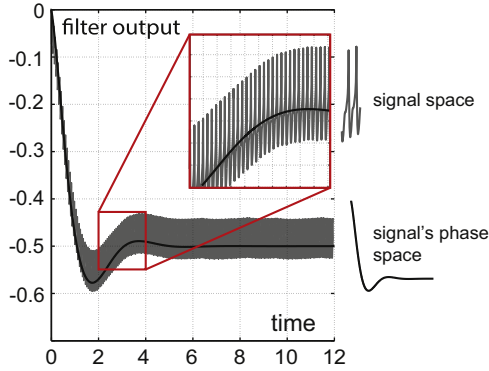
Fig. 7. $\omega_{free}=100.5$ Hz, $\theta_1=100$ Hz, $L=27$, filter transfer functions $1/(s+2)$, sawtooth and triangle waveforms.

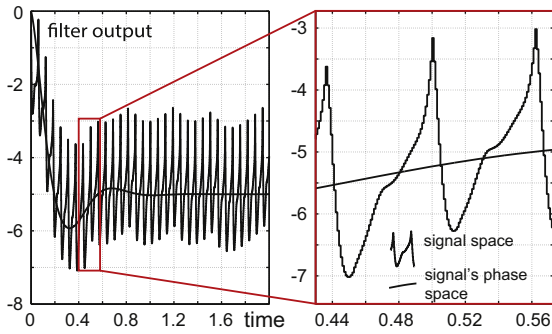**Fig. 8.** $\omega_{free}=105$ Hz, $\theta_1=100$ Hz, $L=100$, analog filter transfer function $1/(0.1s+1)$, discrete filter in z-domain $10/(1-\exp^{-10T}z^{-1})$, sample time 10^{-3}, sawtooth and triangle waveforms.
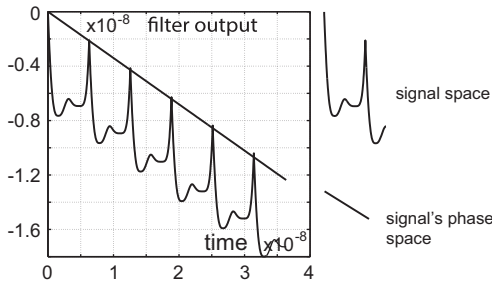

Fig. 9. $\omega_{free}=1000.5$ Hz, $\theta_1=1000$ Hz, $L=27$, filter transfer functions $1/(s+2)$, sawtooth and triangle waveforms.

space only 3.5×10^{-8} s of 10 s of transient process was obtained (see Fig. 9).

These difficulties are described in [37]: "*Direct time-domain simulation of PLLs at the level of SPICE circuits is typically impractical because of its great inefficiency. PLL transients can last hundreds of thousands of cycles, with each cycle requiring hundreds of small time steps for accurate simulation of the embedded voltage-controlled oscillator (VCO). Furthermore, extracting phase or frequency information, one of the chief metrics of PLL performance, from time-*

domain voltage/current waveforms is often difficult and inaccurate."

6. Conclusion

The approach, proposed in this paper, allows one to compute analytically PD characteristics for the general case of periodic waveforms and to construct the nonlinear mathematical model in the signal's phase space for classical Costas loop and, ultimately, to apply numerical simulation and analytical methods (various modifications of absolute stability criteria for pendulum-like systems) for the effective analysis of its stability in the large.

Acknowledgment

Appendix A

A.1. Averaging method

Application of averaging methods [75,76,89,90] requires the consideration of constant data signal and constant frequency of input carrier (20):

$$\theta_1(t)=\omega_1 t+\theta_1(0).$$

In this case (19) is equivalent to

$$\dot{x}=Ax+bf_1(\omega_1 t+\theta_1(0))f_2(\omega_1 t+\theta_1(0)+\theta_\Delta)$$
$$f_1(\omega_1 t+\theta_1(0))f_2\left(\omega_1 t+\theta_1(0)+\theta_\Delta-\frac{\pi}{2}\right),$$
$$\dot{\theta}_\Delta=\omega_\Delta+L(c^*x). \qquad (22)$$

Assuming that input carrier is a high-frequency signal (ω_1 is large), one can consider small parameter

$$\varepsilon=\frac{1}{\omega_1}. \qquad (23)$$

Denote

$$\tau=\omega_1 t. \qquad (24)$$

Then system (22) can be transformed as

$$\frac{dx}{d\tau}=\varepsilon\left(Ax+bf_1(\tau+\theta_1(0))f_2(\tau+\theta_1(0)+\theta_\Delta)\right.$$
$$\left. f_1(\tau+\theta_1(0))f_2\left(\tau+\theta_1(0)+\theta_\Delta-\frac{\pi}{2}\right)\right),$$
$$\frac{d\theta_\Delta}{d\tau}=\varepsilon(\omega_\Delta+L(c^*x)), \qquad (25)$$

and represented in such a way that

$$\frac{dz}{d\tau}=\varepsilon F(z,\tau), \quad z=(x,\theta_\Delta)^*. \qquad (26)$$

In the classical averaging theory such a form of system is

called a standard form. Consider an averaged equation

$$\frac{dy}{d\tau} = \varepsilon \overline{F}(y), \tag{27}$$

where

$$\overline{F}(y) = \frac{1}{P} \int_0^P F(y, \tau) \, d\tau. \tag{28}$$

Suppose D is a bounded domain containing the point $z_0 = (x(0), \theta_\Delta(0))$. Consider solutions $z(\tau, \varepsilon)$ and $y(\tau, \varepsilon)$ with the initial data $z_0 = y_0$. In this case there exists a constant T such that $z(\tau, \varepsilon)$ and $y(\tau, \varepsilon)$ remain in the domain D for $0 \le \tau \le T/\varepsilon$. Define $\varepsilon_{max} = 1/\omega_{min}$.

Consider system of differential equations

$$\frac{dz}{d\tau} = F(\tau, z, \lambda), \tag{29}$$

where z, F are points of n-dimensional Euclidean space E_n, λ is a parameter.

Let function $F(\tau, z, \lambda)$ be real measurable function in $\tau \in [0, T/\varepsilon]$, $z \in D$ for any $\lambda \in \Lambda$, $\lambda_0 \in \Lambda$, where Λ is a domain of E_n.

Theorem 2. *Consider the following system*:

$$\frac{dz}{d\tau} = \varepsilon F(\tau, z). \tag{30}$$

Assume that the right-hand side $F(\tau, z)$ is uniformly bounded and integrals

$$\int_0^\tau \int_c^z F(\tau, x) \, dx \, dt, \quad 0 \le \tau < \infty, \ y \in D \tag{31}$$

are smooth for any fixed $c \in D$; the following limit

$$\lim_{T \to \infty} \frac{1}{T} \int_0^T F(\tau, z) \, d\tau = \overline{F}(z) \tag{32}$$

exists (uniformly with respect to $z \in D$); uniformly with respect to y, r_m:

$$\lim_{T \to \infty} \frac{1}{T} \int_0^T \frac{F_\Delta(\tau, z_1, \ldots, z_i + r_m, \ldots, z_n) - F_\Delta(\tau, z)}{r_m} \, d\tau = 0,$$
$$z + (0, \ldots, 0, r_m, 0, \ldots, 0)^T \in D, \tag{33}$$

where r_m is a decreasing sequence ($r_m \to 0$ while $m \to \infty$), and $F_\Delta = F(\tau, z) - \overline{F}(z)$; $\overline{F}(z)$ are k-Lipschitz functions; solution $y(\tau)$ of the averaged equation (27) for any τ from $0 \le \tau < \infty$ belongs to the domain D together with its ρ-neighborhood, and solution of the (30) with initial conditions $z(0) = y(0)$ is unique.

Then for any $\eta > 0$, $T > 0$ there is an $\varepsilon_0 > 0$, such that for $0 < \varepsilon < \varepsilon_0$ the solution $z(\tau)$ of (30) satisfies

$$|z(\tau) - y(\tau)| < \eta, \quad \tau \in \left[0, \frac{T}{\varepsilon}\right] \tag{34}$$

A.2. Proof of the main theorem

Suppose, $t \in [0, T]$. Consider a difference

$$g(t) - G(t) = \int_0^t \gamma(t - s) \Big[f_1(\theta_1(s)) f_2(\theta_2(s))$$
$$f_1(\theta_1(s)) f_2 \Big(\theta_2(s) - \frac{\pi}{2} \Big) - \varphi(\theta_2(s) - \theta_1(s)) \Big] ds. \tag{35}$$

Let $m \in \mathbb{N}_0$ such that $t \in [m\delta, (m+1)\delta]$. By definition of δ,

one has $m < T/\delta + 1$. The continuity condition implies that $\gamma(t)$ is bounded on $[0, T]$ and $f_1(\theta), f_2(\theta)$ are bounded on $\mathbb{R}$. Since $f_{1,2}(\theta)$ are piecewise differentiable, one gets

$$\int_t^{(m+1)\delta} \gamma(t - s) f_1(\theta_1(s)) f_2(\theta_2(s))$$
$$f_1(\theta_1(s)) f_2 \Big(\theta_2(s) - \frac{\pi}{2} \Big) ds = O(\delta),$$
$$\int_t^{(m+1)\delta} \gamma(t - s) \varphi(\theta_2(s) - \theta_1(s)) \, ds = O(\delta). \tag{36}$$

It follows that (35) can be represented as

$$g(t) - G(t) = \sum_{k=0}^m \int_{[k\delta, (k+1)\delta]} \gamma(t - s)$$
$$\Big[f_1(\theta_1(s)) f_2(\theta_2(s)) f_1(\theta_1(s)) f_2 \Big(\theta_2(s) - \frac{\pi}{2} \Big)$$
$$- \varphi(\theta_2(s) - \theta_1(s)) \Big] ds + O(\delta). \tag{37}$$

Prove now that on each interval $[k\delta, (k+1)\delta]$ the corresponding integrals are equal to $O(\delta^2)$.

Condition (10) implies that on each interval $[k\delta, (k+1)\delta]$ the following relation

$$\gamma(t - s) = \gamma(t - k\delta) + O(\delta), \quad t > s, \ s, t \in [k\delta, (k+1)\delta] \tag{38}$$

is satisfied. Here $O(\delta)$ is independent of k and the relation is satisfied uniformly with respect to t. By (37), (38), and the boundedness of functions $f_1(\theta), f_2(\theta), \varphi(\theta)$ it can be obtained that

$$g(t) - G(t) = \sum_{k=0}^m \gamma(t - k\delta)$$
$$\int_{[k\delta, (k+1)\delta]} \Big[f_1(\theta_1(s)) f_2(\theta_2(s)) f_1(\theta_1(s)) f_2 \Big(\theta_2(s) - \frac{\pi}{2} \Big)$$
$$- \varphi(\theta_2(s) - \theta_1(s)) \Big] ds + O(\delta). \tag{39}$$

Denote

$$\theta_p^k(s) = \theta_p(k\delta) + \dot{\theta}_p(k\delta)(s - k\delta), \quad p = 1, 2. \tag{40}$$

Then for $s \in [k\delta, (k+1)\delta]$, condition (9) yields

$$\theta_p(s) = \theta_p^k(s) + O(\delta). \tag{41}$$

From (8) and the boundedness of derivative $\varphi(\theta)$ on $\mathbb{R}$ it follows that

$$\int_{[k\delta, (k+1)\delta]} |\varphi(\theta_2(s) - \theta_1(s)) - \varphi(\theta_2^k(s) - \theta_1^k(s))| \, ds = O(\delta^2). \tag{42}$$

If $f_1(\theta)$ and $f_2(\theta)$ are continuous on $\mathbb{R}$, then for $f_1(\theta_1(s)) f_2(\theta_2(s)) f_1(\theta_1(s)) f_2(\theta_2(s) - \pi/2)$ the relation

$$\int_{[k\delta, (k+1)\delta]} f_1(\theta_1(s)) f_2(\theta_2(s)) f_1(\theta_1(s)) f_2 \Big(\theta_2(s) - \frac{\pi}{2} \Big) ds$$
$$= \int_{[k\delta, (k+1)\delta]} f_1(\theta_1^k(s)) f_2(\theta_2^k(s))$$
$$f_1(\theta_1^k(s)) f_2 \Big(\theta_2^k(s) - \frac{\pi}{2} \Big) ds + O(\delta^2) \tag{43}$$

is satisfied. Consider why this estimate is valid for the considered class of piecewise-differentiable waveforms. Since conditions (7) and (9) are satisfied and the functions $\theta_{1,2}(s)$ are differentiable and satisfy (8), for all $k = 0, \ldots, m$ there exist sets E_k (the union of sufficiently small neighborhoods of discontinuity points of $f_{1,2}(t)$) such that the relation $\int_{E_k} ds = O(\delta^2)$ is valid, in which case this relation is satisfied uniformly with

respect to k. Then the piecewise differentiability and boundedness of $f_{1,2}(\theta)$ imply relation (43).

By (42) and (43), relation (39) can be rewritten as

$$g(t) - G(t) = \sum_{k=0}^{m} \gamma(t - k\delta) \int_{[k\delta,(k+1)\delta]}$$

$$\left[\left(\sum_{j=1}^{\infty} a_j^1 \, \cos(j\theta_1^k(s)) + b_j^1 \, \sin(j\theta_1^k(s)) \right) \right.$$

$$\left(\sum_{j=1}^{\infty} a_j^1 \, \cos(j\theta_1^k(s)) + b_j^1 \, \sin(j\theta_1^k(s)) \right)$$

$$\left(\sum_{j=1}^{\infty} a_j^2 \, \cos(j\theta_2^k(s)) + b_j^2 \, \sin(j\theta_2^k(s)) \right)$$

$$\left(\sum_{j=1}^{\infty} a_j^2 \, \cos\left(j\theta_2^k(s) - j\frac{\pi}{2}\right) + b_j^2 \, \sin\left(j\theta_2^k(s) - j\frac{\pi}{2}\right) \right)$$

$$\left. - \varphi(\theta_2^k(s) - \theta_1^k(s)) \right] ds + O(\delta). \tag{44}$$

By (14)

$$g(t) - G(t) = \sum_{k=0}^{m} \gamma(t - k\delta) \int_{[k\delta,(k+1)\delta]}$$

$$\left[\left(\sum_{j=1}^{\infty} a_j^1 \, \cos(j\theta_1^k(s)) + b_j^1 \, \sin(j\theta_1^k(s)) \right) \right.$$

$$\left(\sum_{j=1}^{\infty} a_j^1 \, \cos(j\theta_1^k(s)) + b_j^1 \, \sin(j\theta_1^k(s)) \right)$$

$$\left(\sum_{j=1}^{\infty} a_j^2 \, \cos(j\theta_2^k(s)) + b_j^2 \, \sin(j\theta_2^k(s)) \right)$$

$$\left(\sum_{j=1}^{\infty} \alpha_j^2 \, \cos(j\theta_2^k(s)) + \beta_j^2 \, \sin(j\theta_2^k(s)) \right)$$

$$\left. - \varphi(\theta_2^k(s) - \theta_1^k(s)) \right] ds + O(\delta). \tag{45}$$

Since conditions (7)–(9) are satisfied, it is possible to choose $O(1/\delta)$ the sufficiently small time intervals of length $O(\delta^3)$ such that outside this interval the functions $f_p(\theta_p(t))$ and $f_p(\theta_p^k(t))$ are continuous.

It is known that on each interval, which has no discontinuity points, Fourier series of functions $f_1(\theta)$ and $f_2(\theta)$ converge uniformly. Then there exists a number $M = M(\delta) > 0$ such that outside sufficiently small neighborhoods of discontinuity points of $f_p(\theta_p(t))$ and $f_p(\theta_p^k(t))$ the sum of the first M terms of series approximates the original function with an accuracy to $O(\delta)$. In this case by relation (45) and the boundedness of $f_1(\theta)$ and $f_2(\theta)$ on $\mathbb{R}$ it can be obtained:

$$g(t) - G(t) = \sum_{k=0}^{m} \gamma(t - k\delta) \int_{[k\delta,(k+1)\delta]}$$

$$\left[f_1\left(\theta_1^k(s)\right) f_2\left(\theta_2^k(s)\right) f_1\left(\theta_1^k(s)\right) f_2\left(\theta_2^k(s) - \frac{\pi}{2}\right) \right.$$

$$\left. - \varphi(\theta_2^k(s) - \theta_1^k(s)) \right] ds + O(\delta) = \sum_{k=0}^{m} \gamma(t - k\delta) \int_{[k\delta,(k+1)\delta]}$$

$$\left[\left(\sum_{j=1}^{M} a_j^1 \, \cos(j\theta_1^k(s)) + b_j^1 \, \sin(j\theta_1^k(s)) \right) \right.$$

$$\left(\sum_{j=1}^{M} a_j^1 \, \cos(j\theta_1^k(s)) + b_j^1 \, \sin(j\theta_1^k(s)) \right)$$

$$\left(\sum_{j=1}^{M} a_j^2 \, \cos(j\theta_2^k(s)) + b_j^2 \, \sin(j\theta_2^k(s)) \right)$$

$$\left(\sum_{j=1}^{M} \alpha_j^2 \, \cos(j\theta_2^k(s)) + \beta_j^2 \, \sin(j\theta_2^k(s)) \right)$$

$$\left. - \varphi(\theta_2^k(s) - \theta_1^k(s)) \right] ds + O(\delta) \tag{46}$$

Thus,

$$g(t) - G(t) = \sum_{k=0}^{m} \gamma(t - k\delta) \int_{[k\delta,(k+1)\delta]} \left[\sum_{j=1}^{M} \sum_{i=1}^{M} \sum_{l=1}^{M} \sum_{r=1}^{M} \right.$$

$$(a_j^1 \, \cos(j\theta_1^k(s)) + b_j^1 \, \sin(j\theta_1^k(s)))$$

$$(a_i^1 \, \cos(i\theta_1^k(s)) + b_i^1 \, \sin(i\theta_1^k(s)))$$

$$(a_l^2 \, \cos(l\theta_2^k(s)) + b_l^2 \, \sin(l\theta_2^k(s)))$$

$$(\alpha_r^2 \, \cos(r\theta_2^k(s)) + \beta_r^2 \, \sin(r\theta_2^k(s)))$$

$$\left. - \varphi(\theta_2^k(s) - \theta_1^k(s)) \right] ds + O(\delta). \tag{47}$$

Remark that the addends in (47) consist of the product of four coefficients and four trigonometric functions. Apply the formulas of product of sines and cosines to each addend and use Lemma 1 (assertions of Lemmas 1 and 2 are at the end of Appendix), taking into account the conditions of high-frequency property (7)–(9) and the introduced notion (40). Note that the addends in (47) are similar and the types of functions (sin or cos) and coefficients (a, b, α, β) in no way affect the conclusion of Lemma 1 and its proof. Consider, for example, the following addend of sum (47):

$$\sum_{j,i,l,r=1}^{M} a_j^1 \, \cos(j\theta_1^k(s)) a_i^1 \, \cos(i\theta_1^k(s))$$

$$a_l^2 \, \cos(l\theta_2^k(s)) \alpha_r^2 \, \cos(r\theta_2^k(s)). \tag{48}$$

By the relation

$$\cos(\theta_1) \cos(\theta_2) = \frac{1}{2} \left(\cos(\theta_1 + \theta_2) + \cos(\theta_1 - \theta_2) \right) \tag{49}$$

one obtains

$$S = \sum_{j,i,l,r=1}^{M} a_j^1 \, \cos\left(j\theta_1^k(s)\right) a_i^1 \, \cos\left(i\theta_1^k(s)\right) a_l^2 \, \cos\left(l\theta_2^k(s)\right)$$

$$\alpha_r^2 \, \cos\left(r\theta_2^k(s)\right) = \sum_{j,i,l,r=1}^{M} \frac{a_j^1 a_i^1 a_l^2 \alpha_r^2}{8}$$

$$(\cos((i-j)\theta_1^k(s) - (l+r)\theta_2^k(s))$$

$$+ \cos((i+j)\theta_1^k(s) - (l+r)\theta_2^k(s))$$

$$+ \cos((i-j)\theta_1^k(s) + (l-r)\theta_2^k(s))$$

$$+ \cos((i-j)\theta_1^k(s) + (-l+r)\theta_2^k(s))$$

$$+ \cos((i+j)\theta_1^k(s) + (l+r)\theta_2^k(s))$$

$$+ \cos((i+j)\theta_1^k(s) + (l-r)\theta_2^k(s))$$

$$+ \cos((i+j)\theta_1^k(s) + (-l+r)\theta_2^k(s))$$

$$+ \cos((i-j)\theta_1^k(s) + (l+r)\theta_2^k(s))). \tag{50}$$

Consider an integral of this expression over the interval $[k\delta, (k+1)\delta]$. By Lemma 1 and (40) one has

$$\int_{[k\delta,(k+1)\delta]} \cos(\theta_p^k(s)) \, ds = O(\delta^2), \quad p = 1, 2.$$

The use of relations (7) gives the estimate

$$\int_{[k\delta,(k+1)\delta]} a_j^p \, \cos\left(j\theta_p^k(s)\right) ds = \frac{O(\delta^2)}{j^2}, \quad p = 1, 2. \tag{51}$$

Then for the integral of the first addend of (50) over the interval $[k\delta,(k+1)\delta]$ one obtains

$$\int_{[k\delta,(k+1)\delta]} \sum_{j,i,l,r=1}^{M} \frac{a_j^1 a_i^1 a_l^2 \alpha_r^2}{8}$$
$$\left(\cos\left((i+j)\theta_1^k(s)+(l+r)\theta_2^k(s)\right) \right) ds$$
$$= \sum_{j,i,l,r=1}^{M} \frac{O(\delta^2)}{ijlr \max(i+j,l+r)}. \tag{52}$$

Since the series $\sum_{i,j,l,r=1}^{\infty} 1/ijlr \max(i+j,l+r)$ converges $(i+j \geq 2\sqrt{ij}$ and $l+r \geq 2\sqrt{lr})$, the integration over (50) gives

$$\int_{[k\delta,(k+1)\delta]} S\, ds = \int_{[k\delta,(k+1)\delta]} \sum_{j,i,l,r=1}^{M} \frac{a_j^1 a_i^1 a_l^2 \alpha_r^2}{8}$$
$$(\cos((i-j)\theta_1^k(s)-(l+r)\theta_2^k(s))$$
$$+ \cos((i+j)\theta_1^k(s)-(l+r)\theta_2^k(s))$$
$$+ \cos((i-j)\theta_1^k(s)+(l-r)\theta_2^k(s))$$
$$+ \cos((i-j)\theta_1^k(s)+(-l+r)\theta_2^k(s))$$
$$+ \cos((i+j)\theta_1^k(s)+(l-r)\theta_2^k(s))$$
$$+ \cos((i+j)\theta_1^k(s)+(-l+r)\theta_2^k(s))$$
$$+ \cos((i-j)\theta_1^k(s)+(l+r)\theta_2^k(s))) ds + O(\delta^2). \tag{53}$$

From (8) and Lemma 2 (see below) it follows that

$$\int_{[k\delta,(k+1)\delta]} \sum_{\substack{i,j,l,r=1,\\ i+j \neq -l+r}}^{M} \frac{a_j^1 a_i^1 a_l^2 \alpha_r^2}{8} \cos\left((i+j)\theta_1^k(s)+(l-r)\theta_2^k(s)\right) ds$$
$$= \sum_{\substack{i,j,l,r=1,\\ i+j \neq -l+r}}^{M} O\left(\frac{1}{ijlr|i+j+l-r|}\right) = O\left(\delta^2\right). \tag{54}$$

Similarly,

$$\int_{[k\delta,(k+1)\delta]} \sum_{\substack{i,j,l,r=1,\\ i\pm j \neq l+r}}^{M} \frac{a_j^1 a_i^1 a_l^2 \alpha_r^2}{8} \cos\left((i\pm j)\theta_1^k(s)-(l+r)\theta_2^k(s)\right) ds = O\left(\delta^2\right)$$

$$\int_{[k\delta,(k+1)\delta]} \sum_{\substack{i,j,l,r=1,\\ i\pm j \neq l+r}}^{M} \frac{a_j^1 a_i^1 a_l^2 \alpha_r^2}{8} \cos\left((i\pm j)\theta_1^k(s)-(l+r)\theta_2^k(s)\right) ds = O\left(\delta^2\right). \tag{55}$$

The rest of the addends in (53) enter into definition (12) of $\varphi(s)$.

Note that relations (51) and (52) remain true if cos is replaced by sin. Then

$$\int_{[k\delta,(k+1)\delta]} \sum_{\substack{i,j,l,r=1,\\ i\pm j \neq l+r}}^{M} \frac{a_j^1 a_i^1 a_l^2 \alpha_r^2}{8} \sin\left((i\pm j)\theta_1^k(s)-(l+r)\theta_2^k(s)\right) ds = O\left(\delta^2\right),$$

$$\int_{[k\delta,(k+1)\delta]} \sum_{\substack{i,j,l,r=1,\\ i\pm j \neq -l-r}}^{M} \frac{a_j^1 a_i^1 a_l^2 \alpha_r^2}{8} \sin\left((i\pm j)\theta_1^k(s)+(l+r)\theta_2^k(s)\right) ds = O\left(\delta^2\right),$$

$$\int_{[k\delta,(k+1)\delta]} \sum_{\substack{i,j,l,r=1,\\ i\pm j \neq l+r}}^{M} \frac{a_j^1 a_i^1 a_l^2 \alpha_r^2}{8} \sin\left((i\pm j)\theta_1^k(s)-(l-r)\theta_2^k(s)\right) ds = O\left(\delta^2\right)$$

$$\int_{[k\delta,(k+1)\delta]} \sum_{\substack{i,j,l,r=1,\\ i\pm j \neq -l+r}}^{M} \frac{a_j^1 a_i^1 a_l^2 \alpha_r^2}{8} \sin\left((i\pm j)\theta_1^k(s)+(l-r)\theta_2^k(s)\right) ds = O\left(\delta^2\right). \tag{56}$$

Obviously, the changes from $a^{1,2}$ to $b^{1,2}$ and from α^1 to β^1 remain unchanged relations (56). Thus, some addends from (47) satisfy the relations similar to (56) and the rest of the addends enter into $\varphi(s)$. Theorem is proved.

Lemma 1. *For sufficiently large frequencies ω_{min} the following relations*

$$\int_{[k\delta,(k+1)\delta]} \cos\left(j(\omega_{min}s+\psi)\right) ds = \frac{O(\delta^2)}{j},$$
$$\int_{[k\delta,(k+1)\delta]} \sin\left(j(\omega_{min}s+\psi)\right) ds = \frac{O(\delta^2)}{j}, \quad j \in \mathbb{N}, \; k \in \mathbb{N}_0, \tag{57}$$

where $\delta^2 = \omega_{min}^{-1}$, are satisfied.

Lemma 2. *The series $\sum_{i,j,l=1}^{\infty} \sum_{\substack{r=1,\\ j+l \neq -i+r}}^{\infty} 1/ijlr|j+l+i-r|$ and $\sum_{i,j,l=1}^{\infty} \sum_{\substack{r=1,\\ j+l \neq -i+r}}^{\infty} 1/ijlr|j+l-i-r|$ converge.*

References

[1] J. Costas, Synchoronous communications, in: Proceedings of IRE, vol. 44, 1956, pp. 1713–1718.
[2] J.P. Costas, Receiver for Communication System, US Patent 3,047,659, July 1962.
[3] M. Grewal, L. Weill, A. Andrews, Global Positioning Systems, Inertial Navigation, and Integration, Wiley, 2004.
[4] E. Kaplan, C. Hegarty, Understanding GPS: Principles and Applications, Artech House, 2006.
[5] P. Misra, P. Enge, Global Positioning System: Signals, Measurements, and Performance, Ganga-Jamuna Press, 2006.
[6] Y. Shmaliy, GPS-Based Optimal FIR Filtering of clock Models, Electrical Engineering Developments, Nova Science Publishers, 2009.
[7] D. Doberstein, Fundamentals of GPS Receivers: A Hardware Approach, Springer, 2011.
[8] R.D. Stephens, Phase-Locked Loops for Wireless Communications: Digital, Analog and Optical Implementations, Springer, 2002.
[9] M. Pursley, Introduction to Digital Communications, Electrical Engineering Series, Prentice Hall, 2005.
[10] J. Holmes, Spread Spectrum Systems for GNSS and Wireless Communications, Artech House, 2007.
[11] C. Sayre, Complete Wireless Design, Mcgraw-Hill, 2008.
[12] J. Chitode, Communication Theory, Technical Publications, 2009.
[13] G. Kalivas, Digital Radio System Design, Wiley, 2009.
[14] K. Du, N. Swamy, Wireless Communication Systems: From RF subsystems to 4G enabling technologies, Cambridge University Press, 2010.
[15] Y. Wang, W.R. Leeb, A 90 optical fiber hybrid for optimal signal power utilization, Appl. Opt. 26 (19) (1987) 4181–4184, http://dx.doi.org/10.1364/AO.26.004181.
[16] T. Miyazaki, S. Ryu, Y. Namihira, H. Wakabayashi, Optical Costas loop experiment using a novel optical 90 hybrid module and a semiconductor-laser-amplifier external phase adjuster, in: Optical Fiber Communication, Optical Society of America, 1991, p. WH6.
[17] I.B. Djordjevic, M.C. Stefanovic, S.S. Ilic, G.T. Djordjevic, An example of a hybrid system: coherent optical system with Costas loop in receiver-system for transmission in baseband, J. Lightwave Technol. 16 (2) (1998) 177.
[18] I.B. Djordjevic, M.C. Stefanovic, Performance of optical heterodyne PSK systems with Costas loop in multichannel environment for nonlinear second-order PLL model, J. Lightwave Technol. 17 (12) (1999) 2470.
[19] K. Hasegawa, H. Kanetsuna, M. Wakamori, GPS Positioning Method and GPS Reception Apparatus, eP1092987 A2, 2001.
[20] P.S. Cho, Optical phase-locked loop performance in homodyne detection using pulsed and CW LO, in: Optical Amplifiers and Their Applications/Coherent Optical Technologies and Applications, Optical Society of America, 2006, p. JWB24. URL: ⟨http://www.opticsinfobase.org/abstract.cfm?URI=OAA-2006-JWB24⟩.

[21] Y. Hayami, F. Imai, K. Iwashita, Linewidth investigation for Costas loop phase-diversity homodyne detection in digital coherent detection system, in: Asia Optical Fiber Communication and Optoelectronic Exposition and Conference, IEEE, 2008, pp. 1–3.

[22] G.M. Helaluddin, An improved optical Costas loop PSK receiver: simulation analysis, J. Sci. Ind. Res. 67 (2008) 203–208.

[23] N. Nowsheen, C. Benson, M. Frater, Design of a high frequency FPGA acoustic modem for underwater communication, in: OCEANS 2010 IEEE-Sydney, IEEE, 2010, pp. 1–6.

[24] M. Jeruchim, P. Balaban, K. Shanmugan, Simulation of Communication Systems: Modeling, Methodology and Techniques, Information Technology Series, Springer, 2000.

[25] D. Benarjee, PLL Performance, Simulation, and Design, 4th ed. Dog Ear Publishing, 2006.

[26] R.E. Best, Phase-Lock Loops: Design, Simulation and Application, McGraw-Hill, 2007.

[27] D. Pederson, K. Mayaram, Analog Integrated Circuits for Communication: Principles, Simulation and Design, Springer, 2008.

[28] W. Tranter, T. Bose, R. Thamvichai, Basic Simulation Models of Phase Tracking Devices Using MATLAB, Synthesis Lectures on Communications, Morgan & Claypool, 2010.

[29] P. Goyal, X. Lai, J. Roychowdhury, A fast methodology for first-time-correct design of PLLs using nonlinear phase-domain VCO macro-models, in: Proceedings of the 2006 Asia and South Pacific Design Automation Conference, 2006, pp. 291–296. http://dx.doi.org/10.1109/ASPDAC.2006.1594697.

[30] D. Abramovitch, Efficient and flexible simulation of phase locked loops, Part I: simulator design, in: American Control Conference, Seattle, WA, 2008, pp. 4672–4677.

[31] D. Abramovitch, Efficient and flexible simulation of phase locked loops, Part II: post processing and a design example, in: American Control Conference, Seattle, WA, 2008, pp. 4678–4683.

[32] G.A. Leonov, Computation of phase detector characteristics in phase-locked loops for clock synchronization, Dokl. Math. 78 (1) (2008) 643–645.

[33] N.V. Kuznetsov, G.A. Leonov, M.V. Yuldashev, R.V. Yuldashev, Analytical methods for computation of phase-detector characteristics and PLL design, in: Proceedings of ISSCS 2011—International Symposium on Signals, Circuits and Systems, IEEE, 2011, pp. 7–10. http://dx.doi.org/10.1109/ISSCS.2011.5978639.

[34] N.V. Kuznetsov, G.A. Leonov, P. Neittaanmäki, S.M. Seledzhi, M.V. Yuldashev, R.V. Yuldashev, Nonlinear mathematical models of Costas loop for general waveform of input signal, in: Proceedings of IEEE Fourth International Conference on Nonlinear Science and Complexity, NSC 2012, 2012, pp. 109–112. http://dx.doi.org/10.1109/NSC.2012.6304729.

[35] G.A. Leonov, N.V. Kuznetsov, M.V. Yuldahsev, R.V. Yuldashev, Analytical method for computation of phase-detector characteristic, IEEE Trans. Circuits Syst. II: Express Briefs 59 (10) (2012) 633–647, http://dx.doi.org/10.1109/TCSII.2012.2213362.

[36] S. Goldman, Phase-Locked Loops Engineering Handbook for Integrated Circuits, Artech House, 2007.

[37] X. Lai, Y. Wan, J. Roychowdhury, Fast PLL simulation using nonlinear VCO macromodels for accurate prediction of jitter and cycle-slipping due to loop non-idealities and supply noise, in: Proceedings of the 2005 Asia and South Pacific Design Automation Conference, 2005, pp. 459–464.

[38] V. Kroupa, Phase Lock Loops and Frequency Synthesis, John Wiley & Sons, 2003.

[39] B. Razavi, Phase-Locking in High-Performance Systems: From Devices to Architectures, Wiley, 2003.

[40] J. Barry, E. Lee, D. Messerschmitt, Digital Communications, Kluwer Academic Publishers, 2004.

[41] G. Bianchi, Phase-Locked Loop Synthesizer Simulation, McGraw-Hill, 2005.

[42] V. Manassewitsch, Frequency Synthesizers: Theory and Design, Wiley, 2005.

[43] W. Egan, Phase-Lock Basics, Wiley, 2007.

[44] J. Crawford, Advanced Phase-Lock Techniques, Artech House, 2008.

[45] J. Rogers, C. Plett, Radio Frequency Integrated Circuit Design, Artech House, 2010.

[46] J. Klapper, Phase-Locked and Frequency Feedback Systems: Principle and Techniques, Elsevier Science, 2012.

[47] D. Talbot, Frequency Acquisition Techniques for Phase Locked Loops, Wiley, 2012.

[48] G.A. Leonov, N.V. Kuznetsov, M.V. Yuldahsev, R.V. Yuldashev, Computation of phase detector characteristics in synchronization systems, Dokl. Math. 84 (1) (2011) 586–590, http://dx.doi.org/10.1134/S1064562411040223.

[49] F.-J. Chang, S.-H. Twu, S. Chang, Global bifurcation and chaos from automatic gain control loops, IEEE Trans. Circuits Syst. I: Fundam. Theory Appl. 40 (6) (1993) 403–412.

[50] J. Stensby, Phase-Locked Loops: Theory and Applications, Phase-locked Loops: Theory and Applications, Taylor & Francis, 1997.

[51] K. Watada, T. Endo, H. Seishi, Shilnikov orbits in an autonomous third-order chaotic phase-locked loop, IEEE Trans. Circuits Syst. I 45 (9) (1998) 979–983.

[52] J.R.C. Piqueira, L.H.A. Monteiro, Considering second-harmonic terms in the operation of the phase detector for second-order phase-locked loop, IEEE Trans. Circuits Syst. I 50 (6) (2003) 805–809.

[53] A. Suarez, R. Quere, Stability Analysis of Nonlinear Microwave Circuits, Artech House, 2003.

[54] W. Margaris, Theory of the Non-Linear Analog Phase Locked Loop, Springer Verlag, NJ, 2004.

[55] G. Vendelin, A. Pavio, U. Rohde, Microwave Circuit Design Using Linear and Nonlinear Techniques, Wiley, 2005.

[56] J. Kudrewicz, S. Wasowicz, Equations of Phase-Locked Loops: Dynamics on the Circle, Torus and Cylinder, vol. 59, World Scientific, 2007.

[57] C. Wiegand, C. Hedayat, U. Hilleringmann, Non-linear behaviour of charge-pump phase-locked loops, Adv. Radio Sci. 8 (2010) 161–166.

[58] J. Stensby, An exact formula for the half-plane pull-in range of a PLL, J. Frankl. Inst. 348 (4) (2011) 671–684.

[59] B.C. Sarkar, S.S.D. Sarkar, T. Banerjee, Nonlinear dynamics of a class of symmetric lock range DPLLs with an additional derivative control, Signal Process. 94 (2014) 631–641.

[60] C. Chicone, M. Heitzman, Phase-locked loops, demodulation, and averaging approximation time-scale extensions, SIAM J. Appl. Dyn. Syst. 12 (2) (2013) 674–721.

[61] T. Yoshimura, S. Iwade, H. Makino, Y. Matsuda, Analysis of pull-in range limit by charge pump mismatch in a linear phase-locked loop, IEEE Trans. Circuits Syst. I: Reg. Papers 60 (4) (2013) 896–907.

[62] F.H. Henning, Nonsinusoidal Waves for Radar and Radio Communication, Academic Press, 1981.

[63] W. Rosenkranz, Phase-locked loops with limiter phase detectors in the presence of noise, IEEE Trans. Commun. COM 30 (10) (1982) 805–809.

[64] L. Wang, T. Emura, A high-precision positioning servo-controller using non-sinusoidal two-phase type PLL, in: UK Mechatronics Forum International Conference, Elsevier Science Ltd., 1998, pp. 103–108.

[65] P. Sutterlin, W. Downey, A Power Line Communication Tutorial—Challenges and Technologies, Technical Report, Echelon Corporation, 1999.

[66] L. Wang, T. Emura, Servomechanism using traction drive, JSME Int. J. Ser. C 44 (1) (2001) 171–179.

[67] G. Chang, C. Chen, A comparative study of voltage flicker envelope estimation methods, in: Power and Energy Society General Meeting—Conversion and Delivery of Electrical Energy in the 21st Century, 2008, pp. 1–6.

[68] A. Sarkar, S. Sengupta, Second-degree digital differentiator-based power system frequency estimation under non-sinusoidal conditions, IET Sci. Meas. Technol. 4 (2) (2010) 105–114.

[69] F. Gardner, Phase-Lock Techniques, John Wiley, New York, 1966.

[70] A. Viterbi, Principles of Coherent Communications, McGraw-Hill, New York, 1966.

[71] W. Lindsey, Synchronization Systems in Communication and Control, Prentice-Hall, NJ, 1972.

[72] V. Shakhgil'dyan, A. Lyakhovkin, Sistemy fazovoi avtopodstroiki chastoty (Phase Locked Systems), Svyaz', Moscow, 1972 (in Russian).

[73] L. Thede, Practical Analog and Digital Filter Design, Artech House, 2005.

[74] G.A. Leonov, N.V. Kuznetsov, M.V. Yuldashev, R.V. Yuldashev, Differential equations of Costas loop, Dokl. Math. 86 (2) (2012) 723–728, http://dx.doi.org/10.1134/S1064562412050080.

[75] N. Krylov, N. Bogolyubov, Introduction to Non-Linear Mechanics, Princeton University Press, Princeton, 1947.

[76] Y. Mitropolsky, N. Bogolubov, Asymptotic Methods in the Theory of Non-Linear Oscillations, Gordon and Breach, New York, 1961.

[77] G.A. Leonov, N.V. Kuznetsov, Hidden attractors in dynamical systems. From hidden oscillations in Hilbert–Kolmogorov, Aizerman, and Kalman problems to hidden chaotic attractors in Chua circuits, Int. J. Bifurc. Chaos 23 (1), art. no. 1330002. http://dx.doi.org/10.1142/S0218127413300024.

[78] G.A. Leonov, N.V. Kuznetsov, Time-varying linearization and the Perron effects, Int. J. Bifurc. Chaos 17 (4) (2007) 1079–1107, http://dx.doi.org/10.1142/S0218127407017732.

[79] V.A. Yakobovich, G.A. Leonov, A.K. Gelig, Stability of Stationary Sets in Control Systems with Discontinuous Nonlinearities, World Scientific, Singapore, 2004.

[80] N.V. Kuznetsov, Stability and Oscillations of Dynamical Systems: Theory and Applications, Jyvaskyla University Printing House, 2008.

[81] G.A. Leonov, N.V. Kuznetsov, S.M. Seledzhi, Nonlinear analysis and design of phase-locked loops, in: Automation Control—Theory and Practice, In-Tech, 2009, pp. 89–114. http://dx.doi.org/10.5772/7900.

[82] G.A. Leonov, V. Reitmann, V.B. Smirnova, Nonlocal Methods for Pendulum-like Feedback Systems, Teubner Verlagsgesselschaft, Stuttgart-Leipzig, 1992.

[83] G.A. Leonov, D.V. Ponomarenko, V.B. Smirnova, Frequency-Domain Methods for Nonlinear Analysis. Theory and Applications, World Scientific, Singapore, 1996.

[84] F. Tricomi, Integrazione di unequazione differenziale presentatasi in elettrotechnica, Ann. R. Sc. Norm. Super. Pisa 2 (2) (1933) 1–20.

[85] J. Kudrewicz, S. Wasowicz, Equations of Phase-Locked Loop. Dynamics on Circle, Torus and Cylinder, Series A, vol. 59, World Scientific, 2007.

[86] N.V. Kuznetsov, G.A. Leonov, P. Neittaanmäki, S.M. Seledzhi, M.V. Yuldashev, R.V. Yuldashev, Simulation of phase-locked loops in phase-frequency domain, in: International Congress on Ultra Modern Telecommunications and Control Systems and Workshops, IEEE, 2012, pp. 351–356 (art. no. 6459692). http://dx.doi.org/10.1109/ICUMT.2012.6459692.

[87] N.V. Kuznetsov, G.A. Leonov, P. Neittaanmaki, M.V. Yuldashev, R.V. Yuldashev, Method and System for Modeling Costas Loop Feedback for Fast Mixed Signals, Patent Application FI20130124, 2013.

[88] S.A. Tretter, Communication System Design Using DSP Algorithms with Laboratory Experiments for the TMS320C6713TM DSK, Springer, 2007.

[89] A. Samoilenko, R. Petryshyn, Multifrequency Oscillations of Nonlinear Systems, Mathematics and Its Applications, Springer, 2004.

[90] J.A. Sanders, F. Verhulst, J. Murdock, Averaging Methods in Nonlinear Dynamical Systems, Springer, 2007.